Search for New Particles Produced by High-Energy Photons*

A. BARNA, J. COX, F. MARTIN, M. L. PERL, T. H. TAN, W. T. TONER, AND T. F. ZIPF
Stanford Linear Accelerator Center, Stanford University, Stanford, California 94305
AND
E. H. BELLAMY†
High Energy Physics Laboratory, Stanford University, Stanford, California 94305
(Received 5 April 1968)

A search for new particles which might be produced by photons of energy up to 18 GeV is described. No new particles were found. Calculations of the Bethe-Heitler process are described which make it possible to state that this experiment would have detected non-strongly-interacting particles whose mass and lifetime lay in a definite range, did they exist.

I. INTRODUCTION

WE have used the new Stanford linear electron accelerator to search for hitherto unknown elementary particles, particularly for particles which do not have strong interactions. The basic idea behind this search was that through the photoproduction of particle pairs, any charged particle can be created provided it has an antiparticle and that there is sufficient energy in the incident photon. The Stanford linear electron accelerator provides for the first time an intense source of high-energy photons—up to 18 GeV in this experiment. The experiment consisted of a momentum-analyzed secondary beam and a pair of differential gas Čerenkov counters which allowed particles of various masses in that beam to be detected. We were particularly interested in looking for non-strongly-interacting particles, and provision was made separately to detect strongly- and non-strongly-interacting particles.

In any search for new particles, the method of search limits in some ways the properties of the particles that might be found. This experiment was sensitive to charged particles with lifetimes greater than 5×10^{-9} sec, and with a production cross section at least 10^{-7} times that of the muon. Within these limitations, we have not found any new particles. We have made calculations, described in this paper, of the electromagnetic pair production of particles of arbitrary mass and zero spin. The results of these calculations and those of Tsai and Whitis[1] for spin-$\frac{1}{2}$ particles enable us to make the positive statement that if such non-strongly-interacting particles existed with a mass less than that of the proton and a lifetime similar to that of the kaon, we would have detected them.

II. GENERAL CONSIDERATIONS ON THE EXISTENCE OF ELEMENTARY PARTICLES

In our mind, there are two basic problems in elementary-particle physics. One is to understand and to calculate how the particles interact. The other is to learn what particles exist and to formulate rules which limit the possible kinds of particles. The two problems are related. This can be seen most clearly in the case of the strongly-interacting particles. The mesons and the numerous short-lived particles which appear as resonances in the strong interaction seem to be an intimate part of the interaction itself, so that one can expect that a correct theory of the interaction would also explain and predict the multitude of particles.

In the case of the particles which do not interact strongly, the situation is very different. The only known particles are the photon, the electron, the muon, and the two types of neutrinos. There is no understanding of why these particles and no others should exist, although the electromagnetic and weak interactions can be calculated. In particular, there is the puzzle of the existence of both the electron and the muon, particles so dissimilar in mass yet alike in all other aspects. Because the interactions can be calculated, it is possible to postulate the existence of a new particle and to calculate its lifetime and its effect on known processes as a function of its mass. Many authors have done this.[2] However, all such calculations make the basic assumption that no radically new feature enters into the interaction which could alter the result by orders of magnitude. As an example only, consider the effect of strangeness on the strong interaction. The muon-electron problem seems so little understood that some new concept as unlikely as strangeness was, may be required for its solution. We therefore believe that experimental searches for new particles should not be inhibited by preconceived ideas that short lifetimes are to be expected for massive, weakly-interacting particles. These ideas are based on our current understanding of the physics involved. This is true also of estimates of the production of hypothetical particles in specific processes. For example, the fact that K mesons are not observed to decay into heavy muons[3] means that according to

* Work supported by the U. S. Atomic Energy Commission.
† On leave from Westfield College, University of London, London, England.
[1] Y. S. Tsai and V. Whitis, SLAC Users Handbook, Part D (unpublished) and (private communication).
[2] F. E. Low, Phys. Rev. Letters 14, 238 (1965); F. J. M. Farley, Proc. Roy. Soc. (London) A285, 248 (1965); T. D. Lee and C. N. Yang, Phys. Rev. Letters 4, 307 (1960); J. Schwinger, Ann. Phys. (N. Y.) 2, 407 (1957); S. M. Berman *et al.*, Nuovo Cimento 25, 685 (1962).
[3] A. M. Boyarski *et al.*, Phys. Rev. 128, 2398 (1962); E. W. Beier, Ph.D. thesis, University of Illinois, 1966 (unpublished).

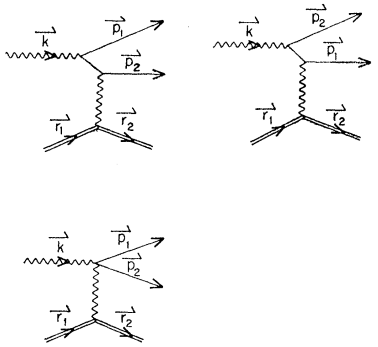

FIG. 1. The three Feynman diagrams upon which are based the calculation of photoproduction of a pair of spin-0 particles.

present understanding of the weak interaction, an exact analog of the muon does not exist with a mass intermediate between that of the muon and the kaon. This is a restricted and specific statement. In the spirit of the foregoing argument, one might then suppose that some additional selection rule or other restriction could exist which would prevent K-meson decay to the heavy muon. It is possible, in this spirit, to conceive of many other particles which might exist, but there is no need to list them here. The purpose of this discussion is to point out that considerations which are of great importance in predicting the effects of specific modifications of present knowledge are limited. Experiments should go beyond the range of such predictions, and be limited only by experimental considerations.

The least specific production process which we can imagine is electromagnetic pair production: It requires only that the particles exist in charged particle-antiparticle pairs. The production rate for this process can be calculated without making further restrictions other than the assumption that effects arising from the form factor of the particle produced can be neglected, so that an experiment using photoproduced particles has a known sensitivity for a general class of particles. A direct search for the particle itself does not introduce any assumption about specific decay modes.

III. OTHER PARTICLE SEARCHES

A. Experiments at Proton Accelerators and with Cosmic Rays

There have been many searches at proton accelerators, mostly unpublished, for new, long-lived, strongly-interacting particles either in beams or in bubble chambers. It is most unlikely that such particles exist in the mass range below $\frac{1}{5}$ GeV. In the case of particles with no strong interaction, the most likely production process is photoproduction by the photons from π^0 decay. However, the photon flux at such machines and in the cosmic radiation is low, and their path length in the target (measured in radiation lengths) is small, so that one can conclude that such searches do not place a useful limit on the existence of non-strongly-interacting particles. The neutrino experiments[4] have placed lower limits to the mass of the hypothetical intermediate boson, a particle of specific properties.

B. Experiments at Electron Machines

Coward *et al.*[5] have searched without success for particles with masses between m_e and $175m_e$. This search was basically similar to the present one in that the particles were photoproduced and detected directly. Definite limits were placed on the mass and lifetime of any particles which could be pair-produced. A short search has been carried out at the Cambridge electron accelerator (CEA) for particles of mass less than the kaon,[6] again without success. Also at CEA, a search has been made for a lepton which could be found in the process $e+p \rightarrow X+p$, in which the recoil proton was momentum-analyzed and a search made for a bump in its momentum spectrum.[7] Again, no new particles were found. These searches cover a limited mass range, or rely on special processes to produce the particles. The present search was intended to cover a wider mass range in a completely general manner.

IV. PARTICLE PRODUCTION BY ELECTRONS

The principal process by which electrons produce secondary charged particles in a thick target takes place in two steps. First, an electron radiates in the Coulomb field of a nucleus. The secondary particles are then photoproduced at another nucleus in the target by the bremsstrahlung. The direct electroproduction reaction $e^-+\text{nucleus} \rightarrow e^-+\text{nucleus}+X^++X^-$, where X^+ and X^- are the particles produced, can be described as photoproduction by virtual photons. It has been shown by Panofsky, Newton, and Yodh[8] that the spectrum of virtual photons associated with an electron is equivalent to the real bremsstrahlung spectrum which would be produced by the electron in a target of 0.02 radiation length. We can therefore neglect this process in a thick target. The photoproduction may be purely electromagnetic pair production, or it may involve the strong interaction. In this section, we describe some calculations of the electromagnetic pair production of spin-0 and spin-$\frac{1}{2}$ particles at 0° in a thick target. The yields to be expected are presented as a function of the mass of the particle produced. These yields represent lower limits for the production of possible new particles under the conditions of our experiment. We have made a number of approximations which we estimate will lead to an over-all error of the order of 20–30% in the yields.

[4] G. Bernardini *et al.*, Nuovo Cimento **38**, 608 (1965); R. Burns *et al.*, Phys. Rev. Letters **15**, 42 (1965).
[5] D. H. Coward *et al.*, Phys. Rev. **131**, 1782 (1963).
[6] J. S. Greenberg (private communication).
[7] C. Betourne *et al.*, Phys. Letters **17**, 70 (1965); H. J. Behrend *et al.*, Phys. Rev. Letters **15**, 900 (1965); R. Budnitz *et al.*, Phys. Rev. **141**, 1313 (1966).
[8] W. K. H. Panofsky, C. M. Newton, and G. B. Yodh, Phys. Rev. **98**, 751 (1955).

TABLE I. The differential cross section at 0° for pair production of a spin-0 particle with 9 GeV/c momentum by a 15-GeV photon incident on a beryllium nucleus, or on a free proton. Values are given for various masses of the produced particle. $|t|_{\min}$ is the minimum value of the square of the four-momentum transfer to the target.

	Beryllium nucleus target			Free proton target	
Particle mass (GeV)	$\lvert t\rvert_{\min}$ (GeV/c)^2	$\frac{1}{Z^2}\left(\frac{d^2\sigma}{d\Omega dp}\right)_{0°}$ cm^2/sr, GeV/c No form factor	cm^2/sr, GeV/c With form factor	$\lvert t\rvert_{\min}$ (GeV/c)^2	$\left(\frac{d^2\sigma}{d\Omega dp}\right)_{0°}$ cm^2/sr, GeV/c With form factor
0.105	2.3×10^{-6}	7.3×10^{-30}	7.0×10^{-30}	2.4×10^{-6}	6.7×10^{-30}
0.20	3.0×10^{-5}	4.2×10^{-31}	3.5×10^{-31}	3.1×10^{-5}	4.1×10^{-31}
0.40	5.0×10^{-4}	1.9×10^{-32}	1.1×10^{-32}	5.1×10^{-4}	1.7×10^{-32}
0.60	2.5×10^{-3}	3.0×10^{-33}	9.5×10^{-34}	2.7×10^{-3}	2.2×10^{-33}
0.80	8.1×10^{-3}	7.9×10^{-34}	1.4×10^{-34}	8.8×10^{-3}	4.4×10^{-34}
1.0	2.0×10^{-2}	2.6×10^{-34}	2.0×10^{-35}	2.3×10^{-2}	1.0×10^{-3}
1.5	0.105	3.1×10^{-35}	3.0×10^{-37}	0.157	2.7×10^{-36}
2.0	0.36	6.1×10^{-36}	7.2×10^{-39}	1.15	3.0×10^{-39}

However, since the yields are a rapidly decreasing function of mass, the effect of such an error is to change only slightly the upper mass limits of the experiment.

We shall now calculate the photoproduction of a pair of spinless particles of mass M and unit charge. Consider first the simplest case, coherent pair production, in which the target nucleus remains in its ground state. The reaction is calculated using the three Feynman diagrams shown in Fig. 1. k is the momentum of the incident photon. E_1, p_1 and E_2, p_2 are the energy and three-momentum of the produced particles, X_1 and X_2. r_1 and r_2 are the initial and final values of the three-momentum of the target nucleus, which has mass M and charge Z. In this experiment, we search for new particles produced at 0±6 mrad to the direction of the incident electron beam. For particles above about 100-MeV mass, the cross section is sufficiently flat in the forward direction that we can use the 0° value. The other particle has spherical angles (θ_2,ϕ_2) with respect to the incident photon direction. The differential cross section[9] in the laboratory system has the form

$$\left(\frac{d^2\sigma}{d\Omega_1 dp_1}\right)_{0°}=\int_0^{2\pi}d\phi_2\int_0^{\pi}\sin\theta_2\,d\theta_2 \times\left|\left(\frac{p_2p_1^2}{2^{10}\pi^5E_1WM(E_2+W)(1-D\cos\theta_2)}\right)\langle|A_0|^2\rangle_{\rm av}\right|. \quad (1)$$

The first term in the brackets is the phase-space factor and the second term is the square of the matrix element. W is the total energy of the recoil nucleus.

$$D=E_2(k-p_1)/p_2(E_2+W).$$

After averaging over the incident photon polarization, the matrix element squared has the form

$$\langle|A_0|^2\rangle_{\rm av}=\frac{Z^2 8M^2E_1^2e^6p_2^2}{k^2t^2E_2^2}\left(\frac{\sin\theta_2}{1-\beta_2\cos\theta_2}\right)^2. \quad (2)$$

The electric charge is defined by $e^2=4\pi\alpha$, where α is the fine-structure constant. β_2 is the laboratory velocity of X_2. t is the square of the four-momentum transferred to the nucleus, defined by

$$t=(k-E_1-E_2)^2-(\mathbf{k}-\mathbf{p}_1-\mathbf{p}_2)^2.$$

Inserting Eq. (2) into Eq. (1) and integrating over ϕ_2 yields

$$\left(\frac{d^2\sigma}{d\Omega_1 dp_1}\right)_{0°,\rm nucl,nff}=\int_0^{\pi}\sin\theta_2\,d\theta_2\left[\left(\frac{Z^2\alpha^3}{\pi}\frac{E_1p_1^2p_2^3M}{k^3E_2^2(E_2+W)(1-D\cos\theta_2)}\right)\times\left(\frac{1}{t^2}\right)\left(\frac{\sin\theta_2}{1-\beta_2\cos\theta_2}\right)^2\right] \quad (3)$$

for the production at 0° of a spin-0 particle. The subscript nff means that no form factor is included.

Consider the production of $m=0.2$ GeV particles by a 15-GeV photon. As θ_2 increases from 0°, the overwhelming variation in the integrand is in the last two terms. The first term, which is mostly the phase-space factor, decreases by 4% as θ_2 goes from 0.0 to 0.2 rad. But $|t|$ increases from 6×10^{-3} (GeV/c)^2 to about 1.2 (GeV/c)^2, which by itself leads to a 4×10^4 decrease in the integrand. The third term is 0 at 0° and reaches a maximum at $\cos\theta_2=\beta_2$. In fact, the integrand is relatively large only in the region where the growth of the last term toward its maximum is not yet canceled by the $1/t^2$ term. Thus the cross section is due primarily to the small four-momentum transfer part of the reaction, 0.01 to 0.2 (GeV/c)^2 in this example.

In the production of much heavier particles, say, $m>0.5$ GeV, the major variation in the integrand of Eq. (3) is in the last two terms, as before. However, we find that we can no longer have very low values of $|t|$.

[9] Equations (1) and (5) were directly derived from the Feynman rules given in J. D. Bjorken and S. D. Drell, *Relativistic Quantum Mechanics* (McGraw-Hill Book Co., New York, 1964), p. 285. Equation (1) when partially integrated agrees with the result of S. D. Drell, Stanford Linear Accelerator Report No. M-200-7A, 1960, p. 7 (unpublished). Equation (1) and the Drell result are exactly equal to one quarter of the cross section given for the coherent production of a pair of spin-0 particles by W. Pauli and V. F. Weisskopf, Helv. Phys. Acta 7, 709 (1934).

TABLE II. The numbers in the table are the ratio of the coherent photoproduction of spin-$\frac{1}{2}$ particles to that of spin-0 particles. The production is on beryllium and the particles are produced at 0° with 9-GeV/c momentum. Values are given for various incident photon energies and various masses for the produced particles.

Mass (GeV)	Incident photon energy (GeV) 18	16	14	12	10
0.105	2.3	2.3	2.7	3.9	5.4
0.20	2.2	2.3	2.7	3.8	10.7
0.40	2.2	2.3	2.6	3.8	11.4
0.60	2.2	2.3	2.6	3.7	12.9
0.80	2.2	2.3	2.6	3.9	16.2
1.0	2.2	2.3	2.7	4.0	
1.5	2.2	2.4	2.9	4.8	
2.0	2.3	2.5	3.3	6.3	

It is easy to see this by considering a very heavy target of mass much greater than the incident photon energy. Then the minimum four-momentum transfer squared is

$$|t|_{\min}=M^4k^2/4p_1^2(k-p_1)^2$$

and $|t|_{\min}$ is proportional to the fourth power of the particle mass. Column 2 of Table I gives $|t|_{\min}$ when beryllium is the target and we have used a 15-GeV incident photon to produce a 9-GeV/c momentum particle. As m goes from 0.105 to 2.0 GeV, $|t|_{\min}$ changes by a factor of 10^5.

Since t^2 enters in the denominator of Eq. (3) and most of the integrand comes from small $|t|$ values, we must expect a strong mass dependence in the cross section. This mass dependence is illustrated in column 3 of Table I. The cross section, divided by Z^2, calculated from Eq. (3) for production of a 0.105-GeV mass particle at 9 GeV/c and 0° by a 15-GeV photon on beryllium is 7.3×10^{-30} cm^2/sr (GeV/c). For a 1.0-GeV mass particle under the same conditions, the cross section, divided by Z^2, is 2.6×10^{-34} cm^2/sr (GeV/c). Thus, even in the simplest case of the production of spin-0 particles from a point nucleus, there is strong mass dependence. The finite size of the nucleus is taken into account by multiplying the cross section by the square of the nuclear form factor.[10] For beryllium, we obtain

$$\left(\frac{d^2\sigma}{d\Omega_1 dp_1}\right)_{0°,\text{nucl}}=\left(\frac{d^2\sigma}{d\Omega_1 dp_1}\right)_{0°,\text{nucl,nff}}\times\left(\frac{1}{1+26.7|t|}\right)^2. \quad (4)$$

Since $|t|_{\min}$ increases with the mass of the particles produced, the form factor reduces further the cross section for the production of massive particles. In column 4 of Table I, the cross section of column 3 is shown, but now with the effect of the nuclear form factor included. For a particle of 1-GeV mass and 9-GeV/c momentum, photoproduced by a 15-GeV photon, the form factor depresses the cross section by a further factor of 10.

This reduction of the coherent pair production requires the consideration of incoherent pair production which results from the interaction of a photon with an individual nucleon in the nucleus. In this process the form factor of the nucleon must be considered. But the nucleon form factor is less $|t|$-dependent than the nuclear form factor. Therefore, as the mass of the particle produced increases, the incoherent production becomes more important. Equation (5) gives a slightly simplified formula[9] for the production cross section of a pair of spin-0 particles on a free proton, in which some terms which are only important for $|t|>1$ (GeV/c)^2 have been neglected.

$$\left(\frac{d^2\sigma}{d\Omega_1 dp_1}\right)_{0°,\text{proton}}=\int_0^\pi \sin\theta_2\, d\theta_2\left\{\left(\frac{\alpha^3}{\pi}\frac{E_1p_1^2p_2^3M}{k^3E_2^2(E_2+W)(1-D\cos\theta_2)}\right)\times\left(\frac{1}{t^2}\right)\left[\left(\frac{G_E^2+|t/4M^2|G_m^2}{1+|t/4M^2|}\right)\left(\frac{\sin\theta_2}{1-\beta_2\cos\theta_2}\right)^2+\frac{G_m^2|t|k^2E_2^2}{2M^2E_1^2p_2^2}\right]\right\}. \quad (5)$$

Comparison of Eq. (5) with Eq. (3) shows the following differences. Of course, Z^2 has been dropped. The last term is now more complicated and contains the nucleon form factors G_E and G_M. We replace G_E and G_M by the formula

$$G_E=G_M/2.793=(1+1.41|t|)^{-2},$$

where $|t|$ is in (GeV/c)^2. With these substitutions, we have calculated the cross section for the production of spin-0 particles on a free proton. For the case of a 15-GeV incident photon producing a 9-GeV/c particle at 0°, we have given the results in Table I in column 6. For masses less than 0.5 GeV, the free proton cross section is almost the same as the nuclear cross section (divided by Z^2) without the nuclear form factor. As the mass increases, the nucleon form factor begins to reduce the proton cross section. But its effect is much less drastic than the effect of the nuclear form factor on the nuclear cross section. Therefore, for masses above 0.5 GeV, the incoherent cross section gains in importance over the coherent.

Incoherent pair production can take place upon neutrons as well as protons. To calculate this, we have used Eq. (5) with $G_E=0$ and G_M given by

$$G_M/1.913=(1+1.41|t|)^{-2}. \quad (6)$$

The total production, coherent and incoherent, is calculated by Eq. (7).

$$\left(\frac{d^2\sigma}{d\Omega_1 dp_1}\right)_{0°}=\left(\frac{Z^2-Z}{Z^2}\right)\left(\frac{d^2\sigma}{d\Omega_1 dp_1}\right)_{0°,\text{nucl}}+Z\left(\frac{d^2\sigma}{d\Omega_1 dp_1}\right)_{0°,\text{proton}}+(A-Z)\left(\frac{d^2\sigma}{d\Omega_1 dp_1}\right)_{0°,\text{neutron}}. \quad (7)$$

[10] R. Hofstadter, Ann. Rev. Nucl. Sci. 7, 231 (1957).

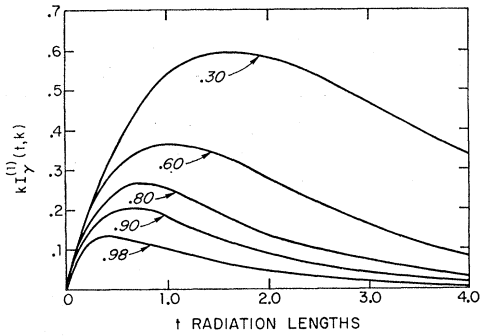

FIG. 2. Bremsstrahlung spectrum as a function of distance along the target t, in radiation lengths. The spectrum is given as the product of the photon energy k in GeV and the photon flux $I_\gamma^{(1)}(t,k)$, in number of photons per GeV. The numbers attached to the curves are the ratio of k to the incident electron energy.

The term $(Z^2-Z)/(Z^2)$, which multiplies the coherent cross section, is a rough way of taking into account the effect of the Pauli principle on the incoherent production.[11] We have used the elastic form factors of the nucleon for G_E and G_M. However, the breakup of the nucleon can also contribute to pair production. Unfortunately, there are as yet insufficient data to allow this to be calculated, and we have therefore neglected it.

All of the foregoing discussion applies to spin-0 particle production. To see the effect of the spins of the produced particles, we will consider the case of the coherent production of spin-$\frac{1}{2}$ particles at 0°. We obtain[12]

$$\left(\frac{d^2\sigma}{d\Omega_1 dp_1}\right)_{0°,\text{nucl,nff}} = \int_0^\pi \sin\theta_2\, d\theta_2 \left[\left(\frac{\alpha^3 Z^2}{\pi}\frac{p_1^2 E_1 p_2^3 M}{k^3 E_2^2 (E_2+M)(1-D\cos\theta_2)}\right) \times\left(\frac{1}{t^2}\right)\left(\frac{\sin^2\theta_2}{1-\beta_2\cos\theta_2}\right)(2) \times\left(\frac{k^2(E_1+p_1)E_2(1-\beta_2\cos\theta_2)}{2E_1^2 m^2}-1\right)\right]. \quad (8)$$

If we compare this to Eq. (3), we see that the spin effect is given by the additional last two terms. Table II shows the effect of these terms by giving the ratio of $d^2\sigma/d\Omega_1 dp_1$ for spin $\frac{1}{2}$ to $d^2\sigma/d\Omega_1 dp_1$ for spin 0, both produced coherently on beryllium at 0°. The calculation included the nuclear form factor as given in Eq. (4). The ratios given in the table are for 10–18-GeV incident photons and a 9-GeV/c momentum secondary particle. When the photon energy is greater by several GeV than the energy of the produced particle, the factor is 2.5 or so. But as the photon energy approaches its threshold value, the factor increases. When the bremsstrahlung spectrum is taken into account, the spin-$\frac{1}{2}$ production is three or four times the spin-0 production at low masses and about two times at high masses.

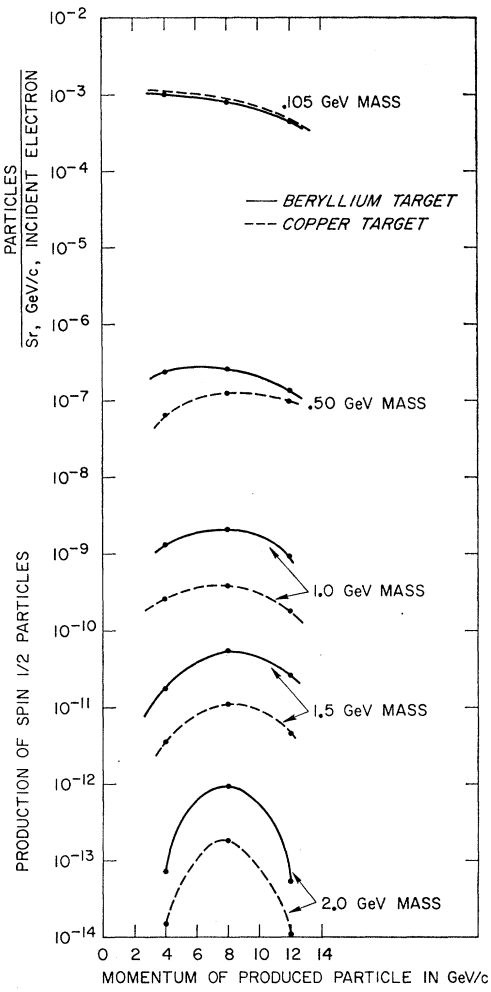

FIG. 3. Photoproduction of pairs of spin-$\frac{1}{2}$ particles by 18-GeV electrons incident on a 10-radiation-length target. The production angle is 0°. The mass number attached to each curve is the mass of the produced particles.

To get the 0° yield of particles from a thick target, we must integrate Eq. (7) over the bremsstrahlung spectrum and the target thickness. The bremsstrahlung spectrum in a thick target has been discussed thoroughly by Tsai and Whitis.[13] For those photons radiated directly by the incident electron (first generation photons), they deduce the approximate expression

$$I_\gamma^{(1)}(t,k) = \frac{1}{k}\frac{(1-k/E_0)^{(4/3)t}\times e^{-(7/9)t}}{7/9+\frac{4}{3}\ln(1-k/E_0)}, \quad (9)$$

where $I_\gamma^{(1)}(t,k)$ is the flux at depth t of first generation photons of energy k due to an electron incident with

[11] S. D. Drell and C. L. Schwartz, Phys. Rev. **112**, 568 (1958).

[12] Equation (8) is obtained by a reduction (setting one particle angle to zero) of the more general equation for the coherent production of a pair of spin-$\frac{1}{2}$ particles. See R. P. Feynman, *Quantum Electrodynamics* (W. A. Benjamin, Inc., New York, 1962), p. 113; W. Heitler, *Quantum Theory of Radiation* (Clarendon Press, Oxford, England, 1954).

[13] Y. S. Tsai and V. Whitis, Phys. Rev. **149**, 1248 (1966).

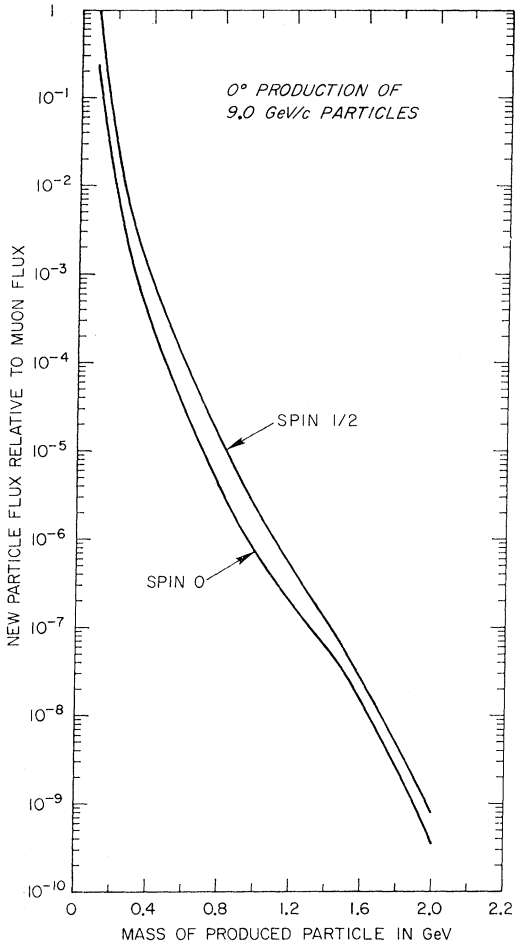

FIG. 4. Ratio of new particle flux to muon flux for various masses, taking the new particle as either spin 0 or spin $\frac{1}{2}$. The flux is for 0° production and 9.0-GeV/c particle momentum from a 10-radiation-length-long beryllium target with 17.5-GeV incident electrons.

energy E_0 at $t=0$. This spectrum is shown in Fig. 2. We make the further approximation of neglecting particle production by the bremsstrahlung of electrons themselves produced in the target by the first generation photons (second generation photons), and all subsequent generations. Tsai and Whitis show that these secondary photons make an appreciable contribution to the spectrum only for large t and small k. Their contribution to the production of high-energy secondary particles can therefore be neglected, and Eq. (9) used directly.

We have calculated the yields for spin-0 particle production by the method described above, and we have used the results of Tsai and Whitis[1] (which are based on a similar method) for spin-$\frac{1}{2}$ particle production. In Fig. 3 are presented their results for the production at 0° of spin $\frac{1}{2}$, pure Dirac particles from a 10-radiation-length target with an incident electron beam energy of 18 GeV. The calculations are presented for both beryllium and copper targets. There are three characteristics of the production which hold equally well for the production of spin-0 particles. First, as we expect, the production decreases rapidly as the mass increases. Second, for larger masses, beryllium is a better target than copper, because the incoherent production is relatively more important in beryllium. Third, the yield has a maximum at roughly half the incident electron momentum.

The most useful way to give the production calculation results is in terms of the ratio of a hypothetical particle flux to the muon flux at a fixed secondary beam momentum. The experimental data were taken at 5.05 and 8.99 GeV/c secondary beam momentum. Figure 4 gives the ratios for 9.0 GeV/c with a 17.5 GeV/c incident electron beam, a 10-radiation-length beryllium target, and 0° production. Results for both spin-$\frac{1}{2}$, pure Dirac particles and spin-0 particles are shown, with masses from 0.1 to 2.0 GeV. Figure 5 gives the ratio of the new particle flux to the muon flux for a secondary-beam momentum of 5.0 GeV/c, for masses below 0.6 GeV, under the same conditions.

V. EXPERIMENTAL METHOD

A. Outline of Method

The experiment is shown schematically in Fig. 6. A 17.5-GeV electron beam struck a thick target. The negative secondaries produced at 0° were formed into a momentum-analyzed beam which passed through two differential gas Čerenkov counters, H and J, set to count particles of a specific velocity, and hence mass. Two counters were used in coincidence in order to give better rejection of unwanted particles. At the end of the beam,

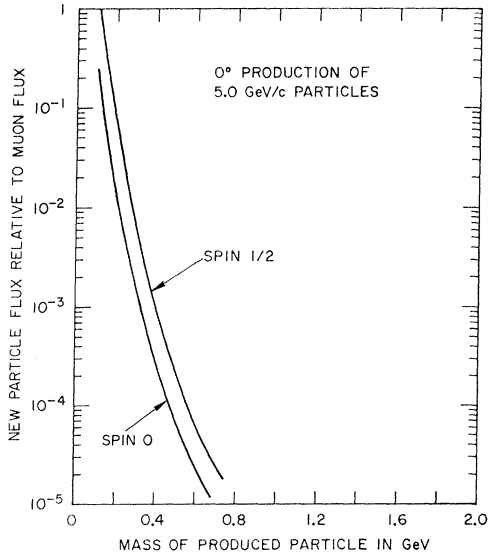

FIG. 5. Ratio of new particle flux to muon flux for various masses, taking the new particle as either spin 0 or spin $\frac{1}{2}$. The flux is for 0° production and 5.0-GeV/c particle momentum from a 10-radiation-length beryllium target with 17.5-GeV incident electrons.

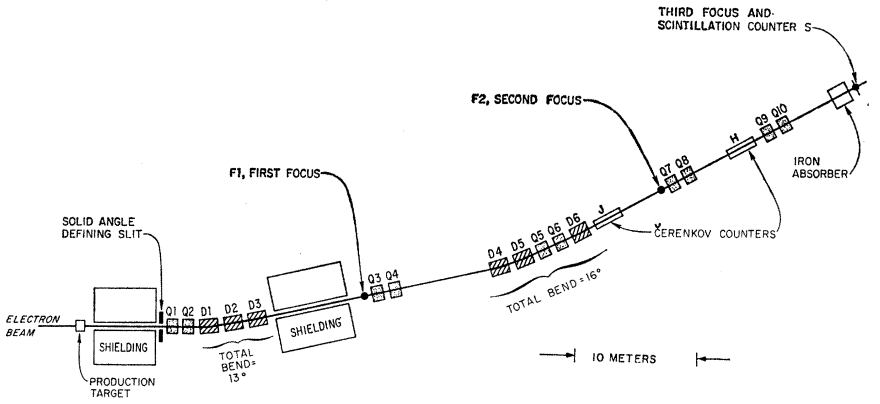

FIG. 6. Schematic diagram of the experiment.

a scintillation counter S was placed behind an iron absorber 5 ft thick. Weakly-interacting particles would have the signature HJS. The experiment consisted of fixing the beam momentum and varying the pressure of the gas in the Čerenkov counters in order to sweep through a range of masses, while recording HJ and HJS. The known particles provide indications of the operation of the system. In particular, the muons and pions provide a basic normalization of the experiment which does not depend upon the acceptance of the transport system or the efficiencies of the Čerenkov counters. Since the muon yield has been measured separately[14] and is understood theoretically, the muon normalization is particularly useful.

B. Apparatus

The target in which the secondaries were produced consisted of 3.6 radiation lengths of beryllium followed by ten radiation lengths of water-cooled copper, a further foot of beryllium, and ten radiation lengths of lead. The production of weakly-interacting particles in this target is adequately described by the calculations given in Sec. IV for production on beryllium, since there is very little particle production beyond the first 3.6 radiation length. The rest of the target was used to absorb the power (up to 20 kW) in the electron beam, and to reduce the number of electrons in the secondary beam to a few percent of the muon flux. Negatively charged secondaries from this target consist mainly of muons and pions. The composition of the beam at momenta of 5.0 and 9.0 GeV/c was measured to be approximately 70% muons, 30% pions.

The beam transport system shown in Fig. 6 was designed and built to provide a muon beam[15] for a muon-scattering experiment. It produces an almost dispersion-free beam in the Čerenkov counters with a diameter of less than 10 cm, a divergence of less than 4 mrad, and a momentum bite of $\pm 1.5\%$. The second focus F2 is 212 ft from the target. Counter J was 19 ft upstream from F2; counter H was 33 ft downstream from F2. The scintillation counter S was at the third focus, 63 ft downstream from F2.

The differential Čerenkov counters were modeled closely on a counter described by Kycia and Jenkins.[16] The present counters are designed to operate at pressures up to 960 psi. In this experiment, CO_2 was used at pressures up to 600 psi. Figure 7(a) is a schematic diagram of a counter. The radiator region is 80 in. long and the counter is designed to be used with beams up to 12.5 cm in diam. Čerenkov light from particles of the correct velocity is focused onto an annular ring aperture. The aperture is split in two across a diameter and the light from each half is collected separately onto two phototubes. A coincidence is required for a particle to be counted. The quartz windows are arranged so that a stray track in the general direction of the beam cannot go through both. Light which falls near, but not on, the annular aperture is reflected from a spherical mirror in which the aperture is set and is collected onto a phototube put in anticoincidence. Without this, a particle of the wrong velocity at an angle to the beam could be counted, as illustrated in Fig. 7(b). The width of the annular aperture was chosen to give an angular acceptance of ± 10 mrad about a mean Čerenkov angle of 75 mrad. This dominated the mass resolution of the counters, giving $\Delta m/m \sim 0.075(p^2/m^2)\times 10^{-2}$, where m is the mass and p is the momentum of the particle. This resolution was adequate to separate out the peaks of the known particles, but allowed a finite mass range to be covered at each pressure setting and sufficient tolerance so that we did not have difficulty in operating the two counters together. The pressure vessels of the two counters were connected together by a common feed pipe. We found that no special precautions were necessary to make the mass peaks coincide in the two counters, although the counters were located out of doors and the ambient temperature varied from 5°C at night to 27°C during the day.

Block diagrams of the electronic circuits are shown in Fig. 8. The three tubes on each counter were fed through

[14] A. Barna *et al.*, Phys. Rev. Letters **18**, 360 (1967).

[15] SLAC Users Handbook, Part D (unpublished); Stanford Linear Accelerator Center Laboratory Report No. SLAC-PUB 434 (unpublished); see also Ref. 13.

[16] T. F. Kycia and E. W. Jenkins, *Nuclear Electronics* (International Atomic Energy Agency, Vienna, 1963).

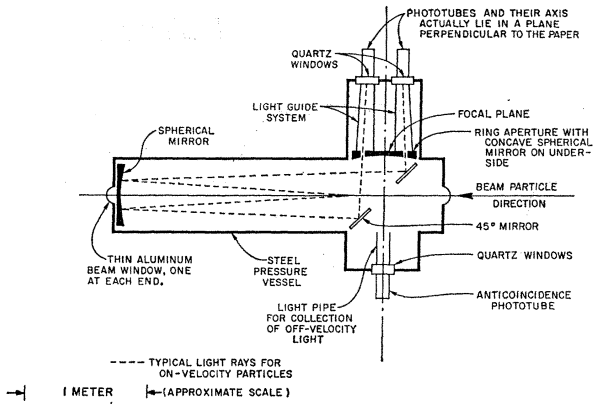

FIG. 7. (a) Schematic diagram of Čerenkov counter optics. (b) Illustration of focal-plane behavior of the Čerenkov light-ring images from different particles.

limiters and discriminators to a coincidence circuit. The discriminator thresholds were set high on the coincidence inputs and low on the veto, following a suggestion of Kycia. This resulted in some inefficiency, but gained more than an order of magnitude in rejection for particles of the wrong velocity. The coincidences HJ and HJS were each formed twice in different ways.

The over-all efficiency of the two counter systems at the π-μ peak was measured to be 80%.

C. Background and Rate Problems

In order to search with high sensitivity, it is necessary to operate at high intensity. A reasonable time to count at one pressure setting is $\frac{1}{2}$ h. This experiment used a pulse repetition rate of 180 pulses/sec, each about 1.2–1.4 μsec long. Thus to search through 10^7 muons in $\frac{1}{2}$ h meant operating with an instantaneous flux of 2.5×10^7 muons/sec. For this reason, we did not define the beam through the Čerenkov counters with scintillators. We used two Čerenkov counters in coincidence, since these are inherently low-rate devices and could be expected to give only those accidental coincidences which resulted from background effects, such as δ rays, off-angle particles, etc., in both counters.

We found a background associated with the kaon and antiproton peaks at the level of about 10^{-7} of the muon flux.

Independently of the S scintillation counter, the maximum usable intensity was limited by the singles rates in the veto phototubes. The light-collection system for the veto operates in such a way that properly aligned beam particles should give veto signals when the pressure is just above or just below the setting required for them to count in the coincidence channel, or when they interact or produce δ rays inclined at an angle to the beam. Otherwise, veto signals should result only from particles at an angle to the axis or with the wrong momentum. We estimated that the veto rate from δ rays should be less than 1% of the flux of pions and muons. However, with the discriminator levels set low on the veto channels, we found that the veto singles rate in each counter was approximately 10% of the beam flux, for pressures far removed from the settings required to count the known particles. We could not raise the discriminator levels without a serious effect on the rejection efficiency of the system. At an instantaneous rate of 2.5×10^7 beam particles/sec, and with veto pulses stretched to 70 nsec for maximum efficiency, the random veto off-time was therefore 33%, and no advantage would be gained by increasing the rate.

VI. EXPERIMENTAL PROCEDURE

The mass range 0.5–1.8 GeV was covered using a beam momentum of 9 GeV/c, roughly half the momentum of the incident electron beam, which the pro-

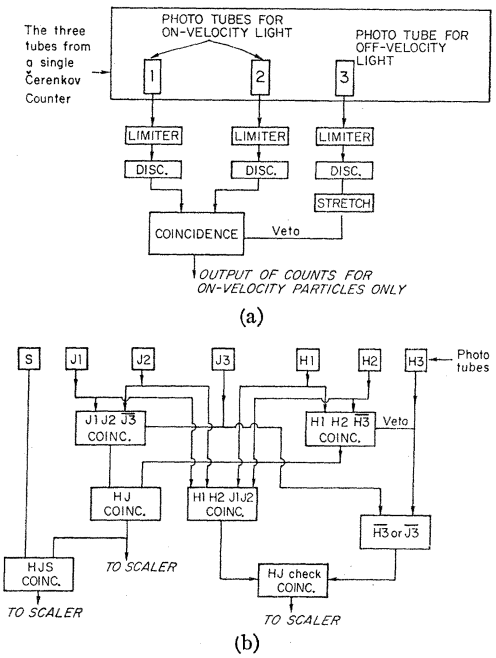

FIG. 8. (a) Schematic diagram of the circuitry used with a single Čerenkov counter; (b) simplified diagram of all the electronics.

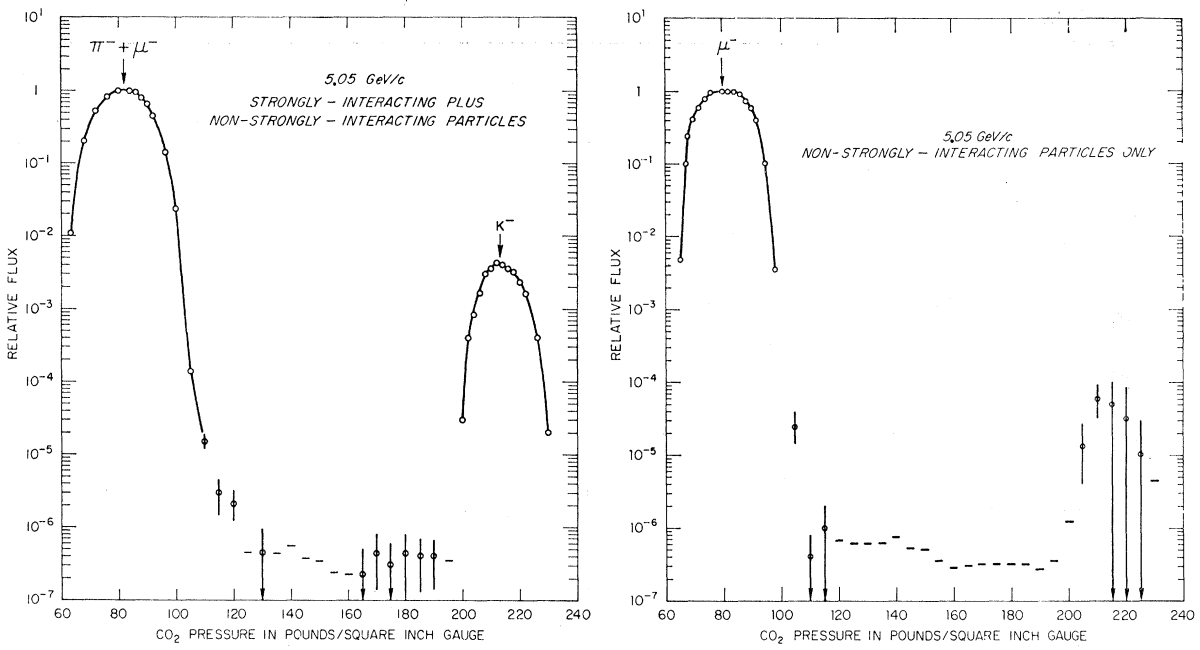

FIG. 9. (a) The flux of strongly-interacting plus non-strongly-interacting particles relative to the pion-plus-muon flux is plotted as a function of the pressure for the 5.05-GeV/c runs. Open circles represent counts and the vertical lines are the statistical errors, which are shown when they are larger than the circle diameter. Short horizontal bars are shown where *no* counts were found. The relative flux indicated by the bar is the flux *if one count* had been seen. At the pion and kaon peak, lines are used to connect the circles to guide the eye. The pressure is in psi gauge. (b) The flux of non-strongly-interacting particles only relative to the muon flux at 5.05 GeV/c. The notation is the same as in (a).

duction calculations showed would give the maximum flux of secondary particles. For the mass range below 0.5 GeV, it was of more importance to have good separation between pions and kaons, and this part of the search was carried out at a momentum of 5 GeV/c.

The process of taking data was relatively simple. The momentum of the secondary beam was fixed at either 9.0 or 5.0 GeV/c. The CO_2 pressure in both counters was set at the muon-pion peak (76–80-psi gauge, depending on the momentum). The timing of all the circuits was checked out and the efficiency of the system for strongly-interacting and non-strongly-interacting particles was determined. Then the pressure was varied from 70 to 100-psi gauge in 4-psi steps across the muon-pion peak. The shapes of the peaks in each counter and of the combined peaks were examined to see that the counters were operating properly. Then the pressure was raised in 5-psi steps. This ensured that at least three steps would be taken to cover the mass peak of any new particle. In each 8-h period of data taking, an upper mass peak (kaon or antiproton) was reached and swept through. This was done to make sure the system was operating properly both with respect to the position and shape of the mass peak. The number of particles per pulse passing through the apparatus was 30–50 during the main part of the data taking between the mass peaks. At the mass peaks, the rate was lower, particularly at the pion-muon peak, where about one particle per pulse was used to reduce dead-time and resolution-time corrections. The number of particles in the beam at these low rates was measured with large auxiliary scintillation counters placed in the beam.

To determine the flux to be used for the normalization of the HJ data at high rates, the singles counts from J1 and H1 were used indirectly. Once off the pion-muon peaks, the J1 or H1 counts were less than 1% of the total number of beam particles, and were observed to be proportional to the beam intensity measured at low rates in the scintillation counters. Therefore, J1 or H1 by themselves had negligible rate corrections. Using the auxiliary beam counters, J1 and H1 were calibrated at very low-beam rates. J1 and H1 were then used as monitors at the high-beam ratios. Of course, this normalization was pressure-dependent, and a calibration was performed regularly. For the HJS channel, dead-time corrections are avoided by normalizing directly to the singles count rate in S. Noise and nonbeam contributions to S singles were observed to be negligible at low rates. Accidental coincidences between HJ and S were monitored by recording coincidences between HJ and a delayed signal from S, and were subtracted.

During the early stages of the experiment, we found that a sensitivity of 10^{-7} relative to the muon flux could be attained, but it would be difficult to go much lower. The limitations were in part due to the maximum allowable muons per pulse being under 50, and in part

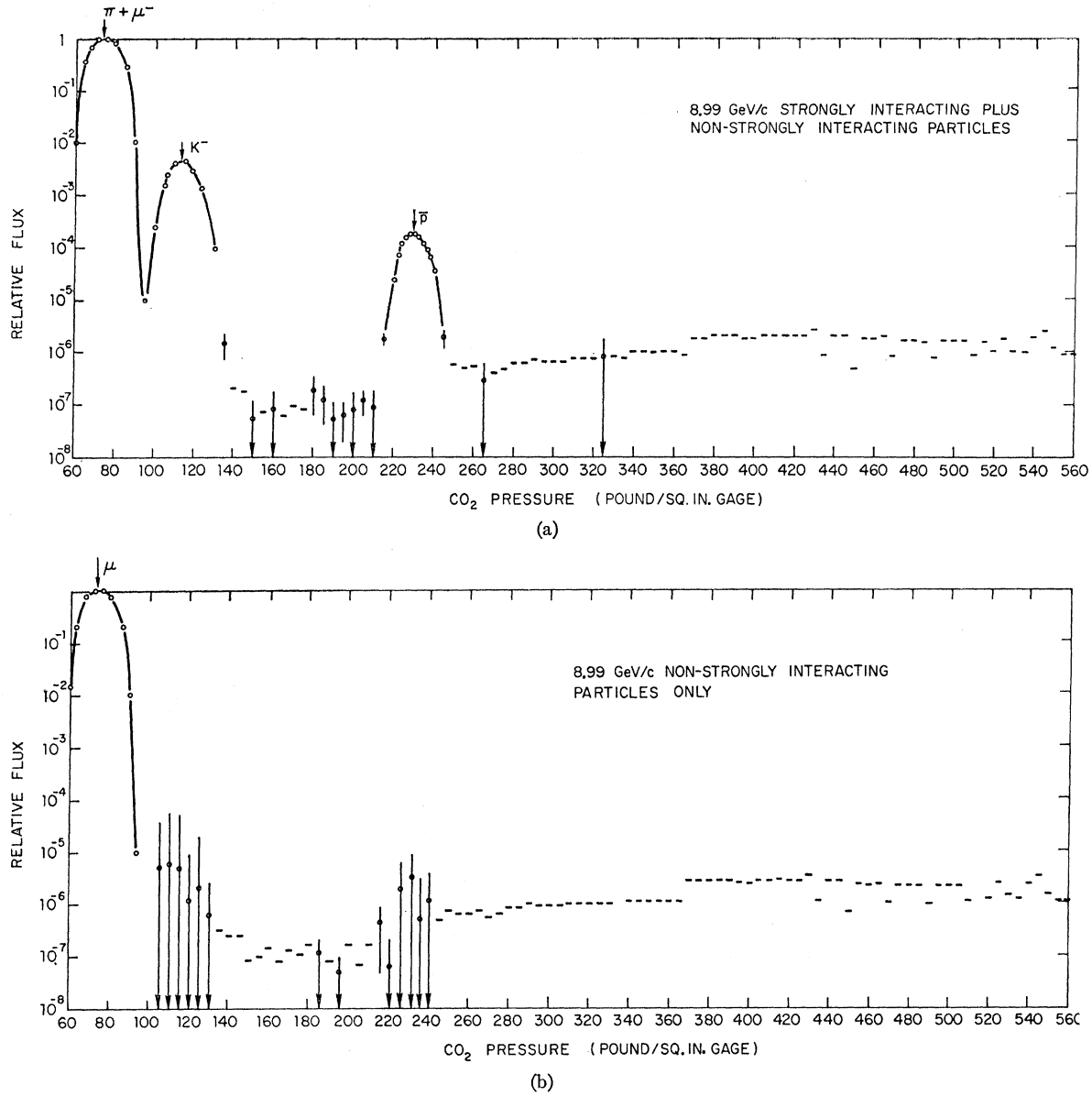

FIG. 10. (a) The flux of a strongly-interacting plus non-strongly-interacting particles relative to the pion-plus-muon flux is plotted as a function of the pressure for the 8.99-GeV/c runs. (b) The flux of non-strongly-interacting particles only relative to the muon flux at 8.99 GeV/c. The notation is the same as in Fig. 9.

due to a background to be discussed in Sec. VII. Now, as shown in Fig. 4, the relative flux of spin-0 particles to muons is 10^{-6} at 0.96-GeV particle mass and 10^{-7} at 1.32-GeV particle mass. We therefore decided to make a definitive search only up to the mass of the proton, i.e., a search in which the sensitivity is considerably better than the flux predicted from purely electromagnetic photoproduction of pairs. Above 1-GeV mass, we made a search with a sensitivity of only 10^{-6} to 3×10^{-6} relative to the muon flux. This part of the search would then depend upon some special mechanism to produce the particles. It was carried out up to a mass of 1.83 GeV. The kinematical mass limit for coherent pair production on beryllium by 17.5 GeV/c photons is 5.4 GeV, and on free protons, 2.3 GeV.

VII. RESULTS AND ANALYSIS

The results presented in this paper are for negative particles. Figure 9(a) shows the combined data for all the 5-GeV/c runs. HJ counts, normalized to the HJ counts at the pion-muon peak, are plotted as a function of pressure. This is called the relative flux. The HJ counts represent the sum of strongly-interacting plus

non-strongly-interacting particles. The notation in the figure has the following meaning. The circles show where counts were found. A vertical line through the circle gives the statistical error, if it is big enough to be shown. The short horizontal lines indicate that no counts were observed at that pressure. If *one* count had been found, the relative flux would be that given by the short horizontal line. The pion-muon and negative kaon peaks have a curve drawn between the circles to guide the eye.

Figure 9(b) shows the relative flux of non-strongly-interacting particles (HJS counts normalized to HJS at the muon peak) at 5 GeV/c. The corresponding results for 9-GeV/c particles are given in Fig. 10. The pion-muon, kaon and antiproton peaks are clearly seen in Fig. 10(a). The notation is the same as that of Fig. 9(a). We make the following observations from Figs. 9 and 10.

(a) The counts observed in Figs. 9(b) and 10(b) at pressures corresponding to the masses of the kaon and antiproton are due to accidental coincidences between the kaons or antiprotons in HJ, and muons in S. The large statistical errors are due to the subtraction of accidental counts from a purposely miss-timed parallel HJS channel. There was no practical way to reduce this accidental rate because at a lower beam intensity it would have taken too long to acquire data. Therefore, we have reduced sensitivity for non-strongly-interacting particles with masses close to the kaon or the antiproton.

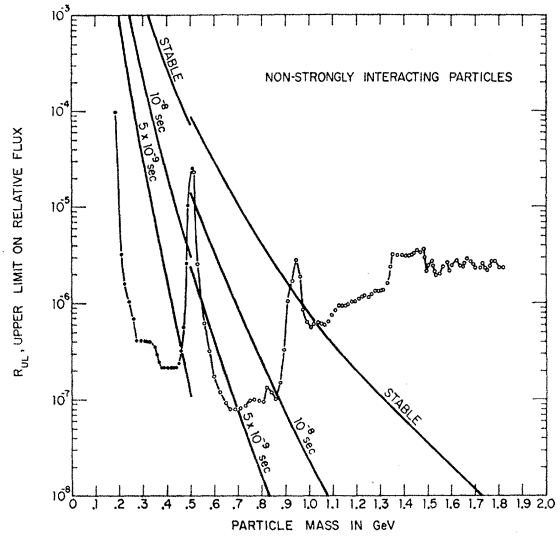

FIG. 11. The upper limit on the relative flux at the apparatus with 90% confidence is plotted against the particle mass in GeV for non-strongly-interacting particles only. The closed circles represent data taken from the 5.05-GeV/c runs and the open circles represent data from 8.99-GeV/c runs. The change comes at 0.5-GeV mass. The slanting lines are the predicted fluxes at the equipment for photoproduction of pairs of spin-0, unit charged, particles which do not *themselves* have form factors. As the notation on the lines indicates, the predicted fluxes are for stable particles, particles with 10^{-8} sec lifetime and particles with 5×10^{-9} sec lifetime. These lines break at 0.5 GeV because of the momentum change.

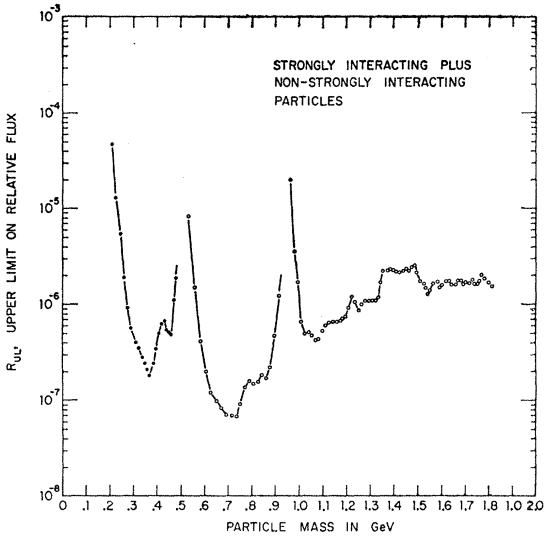

FIG. 12. The upper limit on the relative flux at the apparatus with 90% confidence is plotted against the particle mass in GeV for strongly-interacting plus non-strongly-interacting particles. The closed circles represent data taken from the 5.05-GeV/c runs and the open circles represent data from the 8.99-GeV/c runs.

(b) In Figs. 9(a) and 10(a) there are some counts to the low-mass side of both the kaon and the antiproton peaks, which are not present in Figs. 9(b) and 10(b). Thus, they are due to strongly-interacting particles. Their occurrence in both places makes one suspect a systematic experimental effect. One effect which could explain these counts would be the presence of some 10^{-4} of the kaons in the beam (5×10^{-4} of the antiprotons) with a momentum about 18% higher than the momentum of the beam. The presence of such a small tail of off-momentum particles can certainly not be excluded, although we can find no obvious reason why it should be present.

(c) The search in the region above 240-psi gauge in the 9-GeV/c data involved about 10^8 muons passing through the counters. There were no HJS counts at all in that region. Thus the rejection efficiency for muons is at least 10^8 at high pressures.

In order to compare the data quantitatively with the results of the calculations described in Sec. IV, we have calculated the upper limit which we can put to the relative flux with 90% confidence, using the experimentally observed mass resolution curves to take account of the fact that a particle would give counts at several neighboring pressures if it existed.

Figure 11 summarizes our results for non-strongly-interacting particles. It gives R_{ul}, the upper limit on the relative flux with 90% confidence, as a function of the mass of the particle sought. For 99.9% confidence, the upper limit should increase by a factor of about 5. The curve with solid dots up to about 0.5-GeV mass is from the 5-GeV/c runs. The curve with open circles above 0.5 GeV is from the 9-GeV/c runs. In using these curves.

one must remember that these are upper limits and that their shape depends upon the length of the runs and the background.

The slanted solid lines on the drawing are the predicted relative fluxes using the calculations described in Sec. III. These fluxes are for particles with the following properties: (a) zero spin, (b) unit charge, (c) non-strongly-interacting, and (d) no form factor of the particle itself.

If a particle has spin $\frac{1}{2}$ or higher, or has an anomalous magnetic moment, the production cross section and the relative flux will be greater. Therefore, these lines are the *minimum* relative fluxes for non-strongly-interacting particles with no form factor for the particle itself. The numbers on the slanted lines refer to the lifetime of the particle. The lines are broken at a mass of 0.5 GeV because of the change in momentum at that mass in the experiment.

With Fig. 11, we can make the following conclusions:

(1) There are no stable, unit-charge, non-strongly-interacting particles without form factors in the mass ranges 0.2–0.92 GeV and 0.97–1.03 GeV. By none, we mean that these particles do not exist in pairs capable of electromagnetic pair production.

(2) There are no unit-charge, non-strongly-interacting particles without form factors and with lifetimes greater than 10^{-8} sec in the mass range 0.2–0.86 GeV. There is a small hole in this range at 0.48–0.50 GeV. If the minimum lifetime is reduced to 5×10^{-9} sec, the mass range in which we can be confident that no new particle exists is about 0.2–0.46 and 0.55–0.70 GeV.

(3) Above 1.03 GeV, there could still be stable non-strongly-interacting particles but there is a limit on their production relative to muons. This limit, shown in detail in Fig. 11, ranges from 6×10^{-7} at near 1 GeV to 3×10^{-6} at 1.8 GeV relative to muon production.

(4) No evidence at all was found for the production of any new non-strongly-interacting particles.

Finally, we turn our attention to Fig. 12, which gives R_{ul} for strongly-interacting plus non-strongly-interacting particles. This includes all charged particles in the beam, produced by all sorts of mechanism, and with or without the particles themselves having form factors. It is not useful to put the predicted fluxes from pair photoproduction on this drawing, as was done in Fig. 11, because the strongly-interacting particles can have production cross sections much larger than the pair photoproduction cross section, or they can have smaller production cross sections because of their own form factors. We can only inquire if any new particles are observed.

(5) There is a slight possibility that a hitherto unknown, strongly-interacting particle of mass 0.42 GeV exists, but the evidence is weak and may be due to off-momentum kaons in our beam. If the particle exists, its relative flux was about 4×10^{-7} of the pion plus muon flux in our beam.

(6) There is a very slight possibility that a hitherto unknown, strongly-interacting particle with a mass of 0.8 GeV exists in our beam. However, it is likely that the apparent evidence for this particle is due to high-momentum antiprotons. The particle, if it exists, has a relative flux of 10^{-7} of the pion plus muon flux and is thus just at the edge of the sensitivity of the present experiment.

(7) There is no other evidence for new particles.

There are no earlier published searches for new non-strongly-interacting particles with which our results can be directly compared, because this is the first high-energy photoproduction search. The unpublished results that we have heard of were only qualitative statements that no new particles were seen, but no numerical statements of sensitivity were given.

From our results for strongly-interacting particles, we are able to say only that we did not see any new particles because we cannot predict the production cross section. But for non-strongly-interacting particles without form factors, we have been able to place definite limits of mass and lifetime on particles which could exist. These limits were contained in conclusions (1)–(3).

ACKNOWLEDGMENTS

We are extremely grateful to Dr. Y. S. Tsai for numerous discussions of how to understand and calculate the photoproduction of pairs and for providing us with detailed calculations for the spin-$\frac{1}{2}$ production. We are also very grateful to Dr. T. F. Kycia for providing us with a full set of drawings and advising us in detail of the considerations involved in building and operating the Čerenkov counters. L. Cooper and A. Newton were invaluable in the design and construction of the Čerenkov counters. We appreciate the work of Dr. R. Neal, Dr. E. Seppi, J. Harris and E. Keyser and the accelerator staff in the operation of the accelerator and the experimental areas. We are grateful to R. Vetterlein for the engineering design of the beam.